Inverse Problems **30** (2014) 055002 (20pp)

A novel coupled complex boundary method for inverse source problems

Xiaoliang Cheng[1], Rongfang Gong[2]‡, Weimin Han[3] and Xuan Zheng[1]

[1] Department of Mathematics, Zhejiang University, Hangzhou, Zhejiang 310027, China

[2] Department of Mathematics, Nanjing University of Aeronautics and Astronautics, Nanjing, Jiangsu 211106, China

[3] Department of Mathematics, University of Iowa, Iowa City, IA 52242, USA; School of Mathematics and Statistics, Xi'an Jiaotong University, Xi'an, Shaanxi 710049, China

E-mail: `xiaoliangcheng@zju.edu.cn, grf_math@nuaa.edu.cn, weimin-han@uiowa.edu, zhengxuan@zju.edu.cn`

Abstract. In this paper, we consider an inverse source problem for elliptic partial differential equations with Dirichlet and Neumann boundary data. The unknown source term is to be determined by additional boundary conditions. Unlike the existing methods found in the literature, which usually use some of the boundary conditions to form a boundary value problem for the elliptic partial differential equation and the remaining boundary conditions in the objective functional for optimization to determine the source term, we propose a novel method with coupled complex boundary condition. We use a complex elliptic partial differential equation with a Robin boundary condition coupling the Dirichlet and Neumann boundary data, and optimize with respect to the imaginary part of the solution in the domain to determine the source term. Then, based on the complex boundary value problem, Tikhonov regularization is used for a stable approximate source function and the finite element method is used for discretization. Theoretical analysis is given for both the continuous and discrete models. Several numerical examples are provided to show the usefulness of the proposed coupled complex boundary method.

1. Introduction

Let $\Omega \subset \mathbb{R}^d$ ($d \leq 3$: space dimension) be an open bounded set with boundary $\partial\Omega$, and L be a real linear elliptic differential operator between two Banach spaces. The goal of this paper is to investigate the inverse source problem involving the following equation

$$L\,u = p \quad \text{in } \Omega. \tag{1}$$

Such a problem arises in optical molecular imaging which is currently undergoing a rapid development, see e.g. [20] and references therein for detail. The equation (1) also arises

‡ Corresponding author.

in other applications, such as inverse gravimetry [24], steady heat conduction problems [28, 30], and so on.

The inverse source problem associated with the equation (1) is to identify the right side p in Ω from additional data on the boundary $\partial\Omega$. It is well known that a general source could not be determined uniquely by the boundary measurements, see [23] for a detailed discussion of the theoretical aspects of this problem. From the point of view of mathematics, inverse source problems are under-determined because the boundary $\partial\Omega$ is one dimension lower than the inner domain Ω. Therefore, they are generally ill-posed, i.e. the existence, uniqueness and stability of the solutions are not always guaranteed [18]. This makes solving the problems directly intractable. In the literature, two kinds of strategies are often adopted for obtaining proper approximate solutions. The first one is to provide as much a priori knowledge as possible about the source item p. The a priori information may include permissible regions, some prescribed forms, stronger smoothness assumptions, etc. The famous example in this group is conditional stability, where the source function is sought in a more smooth set [8, 24]. Another widely used strategy for overcoming the ill-posedness is regularization. The regularization methods include Truncated Singular Value Decomposition (TSVD) [24, 26], iterative regularization [3, 5, 11, 26], Tikhonov regularization [5, 6, 11, 12, 24, 26, 33], and so on.

In this paper, we consider using Tikhonov regularization to obtain a stable approximate solution for the inverse source problem associated with the equation (1). For simplicity and clarity of statements, let $L = -\Delta + I$ with I being identical operator. We note that the method developed in our paper can also be applied to more general real linear elliptic differential operators L. For definiteness, in this work, we consider the following inverse source problem.

Inverse source problem. Given g_1 and g_2 on Γ, find p so that the solution of the boundary value problem (BVP)

$$\begin{cases} -\Delta u + u = p\chi_{\Omega_0} & \text{in } \Omega, \\ \frac{\partial u}{\partial n} = g_2 & \text{on } \Gamma \end{cases} \tag{2}$$

satisfies

$$u = g_1 \quad \text{on } \Gamma. \tag{3}$$

Here $\Gamma = \partial\Omega$; $\partial/\partial n$ stands for the outward normal derivative; Ω_0 is known as a permissible region about the source function, and χ_{Ω_0} is the characteristic function of Ω_0, i.e., its value is 1 in Ω_0 and 0 outside Ω_0.

We note that the inverse source problem (2)–(3) has been studied extensively through Tikhonov methods in the field of bioluminescence tomography, see e.g. [7, 14, 20, 21, 29, 31, 34] and references therein. With the Tikhonov regularization, the original inverse source problem (2)–(3) is converted to the following minimization problem:

$$p_\varepsilon = \arg\min_{p \in Q_{ad}} \frac{1}{2}\|u(p) - g_1\|^2_{0,\Gamma} + \frac{\varepsilon}{2}\|p\|^2_{0,\Omega_0}, \tag{4}$$

where Q_{ad} is an admissible set, incorporating a priori information about the source function p; for each p, $u(p)$ is a weak solution of the BVP (2) in the Sobolev space $H^1(\Omega)$. Under some assumptions, Problem (4) admits a unique stable solution p_ε which converges to p^*, a solution of (2)–(3) with minimal L^2-norm ([20]). Regularization with other norms are possible, such as L^1-norm ([22]), BV-norm ([13]), etc.

On the other hand, in [32], a Kohn-Vogelius type functional [2, 25] is used for data fitting. In general, Kohn-Vogelius functionals are expected to lead to more robust optimization procedures [1]. In this case, one is to find a stable approximate source function through the following optimization problem:

$$p_\varepsilon = \arg\min_{p\in Q_{ad}} \frac{1}{2}\|u_1(p) - u_2(p)\|^2_{0,\Omega} + \frac{\varepsilon}{2}\|p\|^2_{0,\Omega_0}, \tag{5}$$

where $u_1(p), u_2(p) \in H^1(\Omega)$ are the weak solutions of BVPs

$$\begin{cases} -\Delta u_1 + u_1 = p\chi_{\Omega_0} & \text{in } \Omega, \\ u_1 = g_1 & \text{on } \Gamma, \end{cases}$$

and

$$\begin{cases} -\Delta u_2 + u_2 = p\chi_{\Omega_0} & \text{in } \Omega, \\ \frac{\partial u_2}{\partial n} = g_2 & \text{on } \Gamma, \end{cases}$$

respectively. Under certain assumptions, Problem (5) admits a unique stable solution p_ε which converges to p^* ([32]).

As we can see from the statements above, both minimization problems (4) and (5) use the Neumann data g_2 and the Dirichlet data g_1 sequentially. In this paper, we propose a novel coupled complex boundary method (CCBM) which uses both data g_1 and g_2 in a single BVP. The idea of CCMB is to couple the Neumann data and Dirichlet data in a Robin boundary condition in such a way that the Neumann data and Dirichlet data are the real part and imaginary part of the Robin boundary condition, respectively. As a result, the data needed to fit is transferred from boundary to interior. Because the BVP is complex, the dimension of the corresponding discrete system increases. Nevertheless, the new method has its own merits and some effective numerical methods could be explored based on our new framework. To the best of our knowledge, in the literature, it is the first time that the idea of the coupled complex boundary condition is explored for solving the inverse source problems.

The paper is organized as follows. A detail statement of CCBM is given in section 2 while some theoretical results about the new regularization framework are reported in section 3. Section 4 is devoted to finite element discretization and corresponding error estimates. In section 5, a simple algorithm is given for practical reconstructions. Several numerical examples are presented in section 6 to demonstrate the feasibility and efficiency of the proposed method. Finally, concluding remarks are given in section 7.

2. A novel coupled complex boundary method

We first introduce notations for function spaces and sets. Assume the boundary $\Gamma = \partial\Omega$ is Lipchitz continuous. For a set G (e.g., Ω, Ω_0 or Γ), we denote by $W^{m,s}(G)$ the standard Sobolev space with norm $\|\cdot\|_{m,s,G}$, $W^{0,s}(G) = L^s(G)$. In particular, $H^m(G)$ represents $W^{m,2}(G)$ with corresponding inner product $(\cdot,\cdot)_{m,G}$ and norm $\|\cdot\|_{m,G}$. Also, let $\mathbf{H}^m(G)$ be the complex version of $H^m(G)$ with inner product $((\cdot,\cdot))_{m,G}$ and norm $|||\cdot|||_{m,G}$ defined as follows: for any $u, v \in \mathbf{H}^m(G)$, $((u,v))_{m,G} = (u,\bar{v})_{m,G}$, $|||v|||^2_{m,G} = ((v,v))_{m,G}$. Set $V = H^1(\Omega)$, $\mathbf{V} = \mathbf{H}^1(\Omega)$, $Q = L^2(\Omega)$, and $\mathbf{Q} = \mathbf{L}^2(\Omega)$. We assume $g_1 \in H^{1/2}(\Gamma)$, $g_2 \in H^{-1/2}(\Gamma)$, and Q_{ad} is a closed convex subset of Q. Finally, we denote by c a constant which may have different value at different place.

Consider a complex BVP

$$\begin{cases} -\Delta u + u = p\chi_{\Omega_0} & \text{in } \Omega, \\ \frac{\partial u}{\partial n} + i\, u = g_2 + i\, g_1 & \text{on } \Gamma, \end{cases} \tag{6}$$

where $i = \sqrt{-1}$ is the imaginary unit. Assume $u = u_1 + i\, u_2 \in \mathbf{V}$ is a weak solution of (6). Then real-value functions $u_1, u_2 \in V$ satisfy

$$\begin{cases} -\Delta u_1 + u_1 = p\chi_{\Omega_0} & \text{in } \Omega, \\ \frac{\partial u_1}{\partial n} - u_2 = g_2 & \text{on } \Gamma, \end{cases} \tag{7}$$

and

$$\begin{cases} -\Delta u_2 + u_2 = 0 & \text{in } \Omega, \\ \frac{\partial u_2}{\partial n} + u_1 = g_1 & \text{on } \Gamma. \end{cases} \tag{8}$$

If $u_2 \equiv 0$ in Ω, then $u_2 \equiv 0$ and $\frac{\partial u_2}{\partial n} \equiv 0$ on Γ. As a result, from BVPs (7) and (8), (u_1, p) is a solution of the original problem (2)–(3). Conversely, if (u, p) is a solution of original problem (2)–(3), then immediately, it satisfies (6).

We conclude from the above discussion that the original inverse source problem is equivalent to the following problem.

Problem 2.1 *Find $p \in Q_{ad}$ such that*

$$u_2 = 0 \text{ in } \Omega,$$

where $u = u_1 + i\, u_2$ solves

$$\begin{cases} -\Delta u + u = p\chi_{\Omega_0} & \text{in } \Omega, \\ \frac{\partial u}{\partial n} + i\, u = g_2 + i\, g_1 & \text{on } \Gamma. \end{cases} \tag{9}$$

Because Problem 2.1 is equivalent to the original inverse source problem, it is ill-posed and regularization is needed for a proper numerical solution. Before regularizing Problem 2.1 , we show a well-posedness result about the BVP (9). To this end, for any $u, v \in \mathbf{V}$, define

$$a(u,v) = \int_\Omega (\nabla u \cdot \nabla \bar{v} + u\,\bar{v})\,\mathrm{d}x + i\int_\Gamma u\,\bar{v}\,\mathrm{d}s,$$
$$f(v) = \int_{\Omega_0} p\,\bar{v}\,\mathrm{d}x + \int_\Gamma g_2\,\bar{v}\,\mathrm{d}s + i\int_\Gamma g_1\,\bar{v}\,\mathrm{d}s.$$

Then the weak form of the BVP (9) is:

$$\text{Find } u \in \mathbf{V} \text{ such that } a(u,v) = f(v) \quad \forall\, v \in \mathbf{V}. \tag{10}$$

Proposition 2.2 *Given $p \in Q$, $g_1 \in L^2(\Gamma)$, $g_2 \in L^{-1/2}(\Gamma)$, the problem (10) admits a unique solution $u \in \boldsymbol{V}$ which depends continuously on p, g_1 and g_2. Moreover,*

$$|||u|||_{1,\Omega} \le c\,(\|p\|_{0,\Omega_0} + \|g_1\|_{1/2,\Gamma} + \|g_2\|_{-1/2,\Gamma}). \tag{11}$$

Proof. We apply the complex version of Lax-Milgram Lemma [10, p. 376] by showing that the antilinear form $a(\cdot,\cdot)$ is continuous and elliptic on $\mathbf{V}$, and the linear form $f(\cdot)$ is continuous on $\mathbf{V}$. Ellipticity of $a(\cdot,\cdot)$ is immediate:

$$\mathrm{Re}\, a(v,v) = \int_\Omega (|\nabla v_1|^2 + v_1^2 + |\nabla v_2|^2 + v_2^2) = |||v|||_{1,\Omega}^2,\ v = v_1 + i\, v_2 \in \mathbf{V}, \tag{12}$$

where $\mathrm{Re}\, a(v,v)$ is the real part of $a(v,v)$. For any $u = u_1 + i\, u_2, v = v_1 + i\, v_2 \in \mathbf{V}$,

$$\begin{aligned} |a(u,v)|^2 = [& \int_\Omega (\nabla u_1 \cdot \nabla v_1 + u_1\, v_1 + \nabla u_2 \cdot \nabla v_2 + u_2\, v_2)\, \mathrm{d}x \\ & + \int_\Gamma (u_1\, v_2 - u_2\, v_1)\, \mathrm{d}s]^2 \\ & + [\int_\Omega (\nabla u_2 \cdot \nabla v_1 + u_2\, v_1 - \nabla u_1 \cdot \nabla v_2 - u_1\, v_2)\, \mathrm{d}x \\ & + \int_\Gamma (u_1\, v_1 + u_2\, v_2)\, \mathrm{d}s]^2. \end{aligned}$$

By applying the Cauchy-Schwarz inequality and the trace inequality, we have the continuity of $a(\cdot,\cdot)$:

$$|a(u,v)| \le c\, |||u|||_{1,\Omega} |||v|||_{1,\Omega}. \tag{13}$$

Similarly, we have the continuity of the linear form $f(\cdot)$:

$$|f(v)| \le c_2\, (\|p\|_{0,\Omega_0} + \|g_1\|_{1/2,\Gamma} + \|g_2\|_{-1/2,\Gamma}) |||v|||_{1,\Omega}. \tag{14}$$

Therefore, the problem (10) admits a unique solution $u \in \mathbf{V}$.

Since $\mathrm{Re}\, a(v,v) \le |a(v,v)|$, (11) follows directly from (10), (12), and (14). ■

Now we are in a position to give a Tikhonov regularization framework for Problem 2.1. For this purpose, for any $p \in Q$, denote by $u := u(p) = u_1(p) + i\, u_2(p) \in \mathbf{V}$ the weak solution of the BVP (9). Moreover, we define a Tikhonov regularization objective functional

$$J_\varepsilon(p) = \frac{1}{2}\|u_2(p)\|_{0,\Omega}^2 + \frac{\varepsilon}{2}\|p\|_{0,\Omega_0}^2,$$

and introduce the following minimization problem:

Problem 2.3 *Find $p_\varepsilon \in Q_{ad}$ such that*

$$J_\varepsilon(p_\varepsilon) = \inf_{p \in Q_{ad}} J_\varepsilon(p).$$

It is not difficult to show

$$\begin{aligned} J'_\varepsilon(p)q &= (u_2(p), u_2(q) - u_2(0))_{0,\Omega} + \varepsilon(p,q)_{0,\Omega_0}, \\ J''_\varepsilon(p)q^2 &= \|u_2(q) - u_2(0)\|^2_{0,\Omega} + \varepsilon\|q\|^2_{0,\Omega_0}. \end{aligned}$$

Hence, for $\varepsilon > 0$, $J_\varepsilon(\cdot)$ is strictly convex.

In the next section, we will give some theoretical results about Problem 2.3.

3. Well-posedness and limiting behavior

We begin with a well-posedness result and the first optimality condition of the solution as follows:

Proposition 3.1 *For any $\varepsilon > 0$, Problem 2.3 has a unique solution $p_\varepsilon \in Q_{ad}$ which depends continuously on all data. Moreover, p_ε is characterized by the inequality*

$$(w_2(p_\varepsilon) + \varepsilon\, p_\varepsilon, q - p_\varepsilon)_{0,\Omega_0} \geq 0 \quad \forall\, q \in Q_{ad}, \tag{15}$$

where $w(p_\varepsilon) = w_1(p_\varepsilon) + i\, w_2(p_\varepsilon) \in \boldsymbol{V}$ is the unique weak solution of adjoint problem:

$$\begin{cases} -\Delta w_\varepsilon + w_\varepsilon = u_2(p_\varepsilon) & \text{in } \Omega, \\ \frac{\partial w_\varepsilon}{\partial n} + i\, w_\varepsilon = 0 & \text{on } \Gamma, \end{cases} \tag{16}$$

and $u(p_\varepsilon) = u_1(p_\varepsilon) + i\, u_2(p_\varepsilon) \in \boldsymbol{V}$ is the weak solution of the BVP (9) with p replaced by p_ε.

Proof. Note that Q_{ad} is a closed and convex set of Hilbert space Q, J_ε is strictly convex. Then, by a standard result on convex minimization problems ([4, 16]), there is a unique stable solution $p_\varepsilon \in Q_{ad}$ to Problem 2.3 and the solution is characterized by the optimality condition

$$J'_\varepsilon(p_\varepsilon)(q - p_\varepsilon) \geq 0 \quad \forall\, q \in Q_{ad}. \tag{17}$$

To prove (15), let $\tilde{u} = u(q) - u(0)$, where $u(q) = u_1(q) + i\, u_2(q)$ and $u(0) = u_1(0) + i\, u_2(0) \in \mathbf{V}$ are weak solutions of the BVP (9), with p replaced by $q \in Q$ and 0 respectively. Then $\tilde{u}$ is the unique weak solution of the BVP:

$$\begin{cases} -\Delta\tilde{u} + \tilde{u} = q\chi_{\Omega_0} & \text{in } \Omega, \\ \frac{\partial\tilde{u}}{\partial n} + i\,\tilde{u} = 0 & \text{on } \Gamma. \end{cases}$$

Multiply (16) with $\tilde{u}$ and integrate by parts to get

$$\int_\Omega u_2(p_\varepsilon)\,(u(q) - u(0))\,\mathrm{d}x = \int_{\Omega_0} w_\varepsilon q\,\mathrm{d}x,$$

i.e.,

$$(u_2(p_\varepsilon), u_2(q) - u_2(0))_{0,\Omega} = (w_2(p_\varepsilon), q)_{0,\Omega_0}.$$

Then the derivative of J_ε at p_ε has the following form: for any $q \in Q$,

$$J'_\varepsilon(p_\varepsilon)q = (w_2(p_\varepsilon) + \varepsilon\, p_\varepsilon, q)_{0,\Omega_0}.$$

Hence, (15) follows from (17). ■

Next we discuss the relation between Problem 2.1 and its regularization Problem 2.3. For this purpose, denote by S the solution set of Problem 2.1, and assume it is nonempty. For example, if Ω is an open bounded set with $C^{1,1}$ boundary Γ, $g_1 \in H^{3/2}(\Gamma), g_2 \in H^{1/2}(\Gamma)$, then Problem 2.1 have infinite many solutions [20, Corollary 2.4]. Moreover, it is straightforward to show that S is closed and convex. Denote by $p_* \in S$ the unique function such that

$$\|p_*\|_{0,\Omega_0} = \inf_{p\in S} \|p\|_{0,\Omega_0}.$$

The next result gives the limiting behavior of p_ε when $\varepsilon \to 0^+$.

Proposition 3.2 *$p_\varepsilon \to p_*$ in Q, as $\varepsilon \to 0^+$.*

Proof. Write $u(p_*) = u_1(p_*) + i\, u_2(p_*) \in \mathbf{V}$, the weak solution of the BVP (9) with p replaced by p_*. Then $u_2(p_*) = 0$ and

$$J_\varepsilon(p_\varepsilon) = \frac{1}{2}\int_\Omega u_2(p_\varepsilon)^2 \mathrm{d}x + \frac{\varepsilon}{2}\int_{\Omega_0} p_\varepsilon^2\, \mathrm{d}x \le J_\varepsilon(p_*) = \frac{\varepsilon}{2}\int_{\Omega_0} p_*^2\, \mathrm{d}x.$$

Thus, $\|p_\varepsilon\|_{0,\Omega_0} \le \|p_*\|_{0,\Omega_0}$. Denote by $u_\varepsilon := u(p_\varepsilon) = u_1(p_\varepsilon) + i\, u_2(p_\varepsilon) \in \mathbf{V}$ the weak solution of the BVP (9) with p replaced by p_ε. Then from (11), we have

$$\begin{aligned} |||u_\varepsilon|||_{1,\Omega} &\le c\,(\|p_\varepsilon\|_{0,\Omega_0} + \|g_1\|_{1/2,\Gamma} + \|g_2\|_{-1/2,\Gamma}) \\ &\le c\,(\|p_*\|_{0,\Omega_0} + \|g_1\|_{1/2,\Gamma} + \|g_2\|_{-1/2,\Gamma}). \end{aligned}$$

Similarly, denote by $w_\varepsilon := w(p_\varepsilon) = w_1(p_\varepsilon) + i\, w_2(p_\varepsilon) \in \mathbf{V}$ the unique weak solution of corresponding adjoint problem (16). Then

$$|||w_\varepsilon|||_{1,\Omega} \le c\,\|u_2(p_\varepsilon)\|_{0,\Omega} \le c\,(\|p_*\|_{0,\Omega_0} + \|g_1\|_{1/2,\Gamma} + \|g_2\|_{-1/2,\Gamma}).$$

Thus, $\{p_\varepsilon\}$, $\{u_\varepsilon\}$ and $\{w_\varepsilon\}$ are uniformly bounded w.r.t. ε in the spaces Q and $\mathbf{V}$ respectively. Therefore, there are some elements $p_0 \in Q$, $u_0 \in \mathbf{V}$, $w_0 \in \mathbf{V}$, and a subsequence $\{\varepsilon'\}$ of $\{\varepsilon\}$ such that, as $\varepsilon' \to 0^+$,

$$\begin{aligned} &p_{\varepsilon'} \rightharpoonup p_0 \text{ in } Q, \quad u_{\varepsilon'} \rightharpoonup u_0, w_{\varepsilon'} \rightharpoonup w_0 \text{ in } \mathbf{V}, \\ &u_{\varepsilon'} \to u_0, w_{\varepsilon'} \to u_0 \text{ in } \mathbf{L}^2(\Omega) \text{ and } \mathbf{L}^2(\Gamma). \end{aligned}$$

Using these convergence relations, we verify that $u_0 = u(p_0) = u_1(p_0) + i\, u_2(p_0)$ and $w_0 = w(p_0) = w_1(p_0) + i\, w_2(p_0)$. Replace ε by ε' in (15) and let $\varepsilon' \to 0^+$ to get

$$(w_2(p_0), q - p_0)_{0,\Omega_0} \ge 0 \quad \forall\, q \in Q_{ad},$$

implying that p_0 is a solution of Problem 2.3 with $\varepsilon = 0$, i.e., a solution of Problem 2.1. So $p_0 \in S$. Also, we have

$$||p_0||_{0,\Omega_0} \le \liminf_{\varepsilon'\to 0^+} ||p_{\varepsilon'}||_{0,\Omega_0} \le ||p_*||_{0,\Omega_0}.$$

By the definition of p_*, we have $p_0 = p_*$. Since the limit p_0 is unique, the entire family p_ε converges weakly to p_* in Q as $\varepsilon \to 0^+$. Consequently, when $\varepsilon \to 0^+$, we have

$$\begin{aligned} ||p_\varepsilon - p_*||^2_{0,\Omega_0} &= ||p_\varepsilon||^2_{0,\Omega_0} - 2\,(p_\varepsilon, p_*)_{0,\Omega_0} + ||p_*||^2_{0,\Omega_0} \\ &\le 2||p_*||^2_{0,\Omega_0} - 2\,(p_\varepsilon, p_*)_{0,\Omega_0} \to 0 \end{aligned}$$

which shows the strong convergene of p_ε to p_* in Q as $\varepsilon \to 0^+$. ■

4. Finite element approximation

In this section, we discretize Problem 2.3 and explore convergence property of the numerical solutions. We use linear finite elements to solve the BVP (9). For the source function p, piecewise constant functions are used. Moreover, for later use of error estimation, in this section, assume $g_1, g_2 \in H^{1/2}(\Gamma)$, and $\Omega \subset \mathbb{R}^d$ is a bounded open set with the boundary $\Gamma \in C^{1,1}$.

Let $\{\mathcal{T}_h\}_h$ be a regular family of finite element partitions of $\overline{\Omega}$ with meshsize h, such that each element at the boundary Γ has at most one non-straight face (for a three-dimensional domain) or side (for a two-dimensional domain). Define the linear finite element space

$$V^h = \{v \in C(\overline{\Omega}) \mid v \text{ is linear in } T \ \forall\, T \in \mathcal{T}_h\}$$

and denote by $\pi^h v$ the piecewise linear interpolant of $v \in H^2(\Omega)$. Then we have the existence of a constant $c > 0$ such that (see [9] for a polyhedral/polygonal domain and [20] for a general smooth domain)

$$\|v - \pi^h v\|_{0,\Omega} + h\|v - \pi^h v\|_{1,\Omega} \le c\, h^2 \|v\|_{2,\Omega} \quad \forall\, v \in H^2(\Omega). \tag{18}$$

Set $\mathbf{V}^h = V^h \oplus iV^h$. Then $\mathbf{V}^h$ is a finite element subspace of $\mathbf{V}$, and the finite element approximation of the BVP (9) is as follows:

$$\text{Find } u^h \in \mathbf{V}^h \text{ such that } a(u^h, v^h) = f(v^h) \quad \forall\, v^h \in \mathbf{V}^h. \tag{19}$$

Similar to Proposition 2.2, the discrete problem (19) admits a unique solution $u^h \in \mathbf{V}^h$.

Next we bound the error $u - u^h$. To this end, we first show a regularity result of the solution $u = u_1 + i\, u_2$. Note that $u_1 \in V$ and $u_2 \in V$ are weak solutions of the BVPs

$$\begin{cases} -\triangle u_1 + u_1 = p\chi_{\Omega_0} & \text{in } \Omega, \\ \frac{\partial u_1}{\partial n} = u_2 + g_2 & \text{on } \Gamma, \end{cases}$$

and

$$\begin{cases} -\triangle u_2 + u_2 = 0 & \text{in } \Omega, \\ \frac{\partial u_2}{\partial n} = g_1 - u_1 & \text{on } \Gamma, \end{cases}$$

respectively. With γ being the standard trace operator, $\gamma u_2 + g_2 \in H^{1/2}(\Gamma)$ and $g_1 - \gamma u_1 \in H^{1/2}(\Gamma)$. Then, we have $u_1, u_2 \in H^2(\Omega)$ ([15, Proposition 2.5.2.3]) and the following bounds ([15, Theorem 2.3.3.2]):

$$\|u_1\|_{2,\Omega} \le c\,(\|p\|_{0,\Omega_0} + \|u_2 + g_2\|_{1/2,\Gamma} + \|u_1\|_{1,\Omega}),$$
$$\|u_2\|_{2,\Omega} \le c\,(\|g_1 - u_1\|_{1/2,\Gamma} + \|u_2\|_{1,\Omega}).$$

Using these bounds and (11), we further deduce that

$$\|u_1\|_{2,\Omega} \le c\,(\|p\|_{0,\Omega_0} + \|g_1\|_{1/2,\Gamma} + \|g_2\|_{1/2,\Gamma}),$$
$$\|u_2\|_{2,\Omega} \le c\,(\|p\|_{0,\Omega_0} + \|g_1\|_{1/2,\Gamma} + \|g_2\|_{1/2,\Gamma}),$$

or

$$|||u|||_{2,\Omega} \le c\,(\|p\|_{0,\Omega_0} + \|g_1\|_{1/2,\Gamma} + \|g_2\|_{1/2,\Gamma}). \tag{20}$$

Now we can derive the a priori finite element error estimates as follows.

Theorem 4.1 *For any $p \in Q$, let $u \in \boldsymbol{V}$ and $u^h \in \boldsymbol{V}^h$ be the solutions of the problems (10) and (19). Then*

$$|||u - u^h|||_{1,\Omega} \le c\, h\, (\|p\|_{0,\Omega_0} + \|g_1\|_{1/2,\Gamma} + \|g_2\|_{1/2,\Gamma}), \tag{21}$$

$$|||u - u^h|||_{0,\Omega} \le c\, h^2\, (\|p\|_{0,\Omega_0} + \|g_1\|_{1/2,\Gamma} + \|g_2\|_{1/2,\Gamma}). \tag{22}$$

Proof. Because $\mathrm{Re}\, a(u,u) = |||u|||^2_{1,\Omega}$ and $a(u - u^h, v^h) = 0$ for any $v^h \in \mathbf{V}^h$, Cea's inequality holds for the approximation of the complex problem (10) by (19); that is, there is a constant c independent of h such that

$$|||u - u^h|||_{1,\Omega} \le c \inf_{v^h \in \mathbf{V}^h} |||u - v^h|||_{1,\Omega}. \tag{23}$$

Notice that for any $v = v_1 + i\, v_2 \in \mathbf{H}^2(\Omega)$, $(\pi^h v_1 + i\, \pi^h v_2) \in \mathbf{V}^h$. Then by (18),

$$\begin{aligned} |||v - (\pi^h v_1 + i\, \pi^h v_2)|||^2_{1,\Omega} &= \|v_1 - \pi^h v_1\|^2_{1,\Omega} + \|v_2 - \pi^h v_2\|^2_{1,\Omega} \\ &\le c_1\, h^2 \|v_1\|^2_{2,\Omega} + c_2\, h^2 \|v_2\|^2_{2,\Omega} \le c\, h^2 |||v|||^2_{2,\Omega}. \end{aligned} \tag{24}$$

We combine (20), (23) and (24) to obtain (21).

As for (22), since $\mathbf{V}$ can be embedded continuously into $\mathbf{Q}$, with similar arguments to those of Aubin-Nitsche lemma ([9, Theorem 3.2.4]), we have

$$|||u - u^h|||_{0,\Omega} \le c\, |||u - u^h|||_{1,\Omega} \sup_{b \in \mathbf{Q}} \{ \frac{1}{|||b|||_{0,\Omega}} \inf_{v^h \in \mathbf{V}^h} |||\varphi_b - v^h|||_{1,\Omega} \}, \tag{25}$$

where $\varphi_b = \varphi_{b,1} + i\, \varphi_{b,2} \in \mathbf{V}$ is the unique solution of the problem

$$a(v, \varphi_b) = ((v, b))_{0,\Omega} \quad \forall\, v \in \mathbf{V};$$

the solution φ_b satisfies

$$|||\varphi_b|||_{1,\Omega} \le |||b|||_{0,\Omega}. \tag{26}$$

Then $\varphi_{b,1} \in V$ and $\varphi_{b,2} \in V$ are weak solutions of BVPs

$$\begin{cases} -\Delta \varphi_{b,1} + \varphi_{b,1} = b_1 & \text{in } \Omega, \\ \frac{\partial \varphi_{b,1}}{\partial n} = -\varphi_{b,2} & \text{on } \Gamma, \end{cases}$$

and

$$\begin{cases} -\Delta \varphi_{b,2} + \varphi_{b,2} = -b_2 & \text{in } \Omega, \\ \frac{\partial \varphi_{b,2}}{\partial n} = \varphi_{b,1} & \text{on } \Gamma, \end{cases}$$

respectively. Again, by applying [15, Proposition 2.5.2.3] and [15, Theorem 2.3.3.2], we have $\varphi_{b,1}, \varphi_{b,2} \in H^2(\Omega)$, and

$$\|\varphi_{b,1}\|_{2,\Omega} \le c\, (\|b_1\|_{0,\Omega} + \|\varphi_{b,2}\|_{1/2,\Gamma} + \|\varphi_{b,1}\|_{1,\Omega}),$$

$$\|\varphi_{b,2}\|_{2,\Omega} \le c\, (\|b_1\|_{0,\Omega} + \|\varphi_{b,1}\|_{1/2,\Gamma} + \|\varphi_{b,2}\|_{1,\Omega}).$$

Recalling (26), we then have

$$|||\varphi_b|||_{2,\Omega} \le c\, |||b|||_{0,\Omega}.$$

Take $v^h = \pi^h \varphi_{b,1} + i\, \pi^h \varphi_{b,2} \in \mathbf{V}^h$ in (25), and use (24) to get

$$|||u - u^h|||_{0,\Omega} \le c\, h\, |||u - u^h|||_{1,\Omega}. \tag{27}$$

The estimate (22) follows from (21) and (27). ■

Now we are in a position to discretize the regularized reconstruction model Problem 2.3. For this purpose, define a discrete regularized objective functional

$$J_\varepsilon^h(p) = \frac{1}{2}\|u_2^h(p)\|_{0,\Omega}^2 + \frac{\varepsilon}{2}\|p\|_{0,\Omega_0}^2,\ p \in Q.$$

Again, it is easy to verify that for $\varepsilon > 0$, $J_\varepsilon^h(\cdot)$ is strictly convex.

For a full discretization of Problem 2.3, we approximate the source function p with piecewise constants. Define

$$Q^h = \{p \in Q \mid p \text{ is constant in } T,\ \forall\ T \in \mathcal{T}_h \text{ and } T \subset \overline{\Omega}_0\}$$

and the orthogonal projection operator $\Pi^h : Q \to Q^h$ by

$$(\Pi^h p, q^h)_{0,\Omega_0} = (p, q^h)_{0,\Omega_0} \quad \forall\, p \in Q,\ q^h \in Q^h. \tag{28}$$

Then it is well-known that

$$\|p - \Pi^h p\|_{0,\Omega_0} \le c\, h\, |p|_{1,\Omega_0} \quad \forall\, p \in H^1(\Omega_0). \tag{29}$$

Set $Q_{ad}^h = Q^h \cap Q_{ad}$ and introduce the following discrete optimization problem:

Problem 4.2 *Find $p_\varepsilon^h \in Q^h$ such that*

$$J_\varepsilon^h(p_\varepsilon^h) = \inf_{p^h \in Q_{ad}^h} J_\varepsilon^h(p^h).$$

Similar to Proposition 3.1, we have the following result on Problem 4.2.

Proposition 4.3 *For any $\varepsilon > 0$, Problem 4.2 has a unique solution $p_\varepsilon^h \in Q^h$ which depends continuously on all data. Moreover, p_ε^h is characterized by*

$$(w_2^h(p_\varepsilon^h) + \varepsilon\, p_\varepsilon^h, q^h - p_\varepsilon^h)_{0,\Omega_0} \ge 0 \quad \forall\, q^h \in Q_{ad}^h, \tag{30}$$

where $w_\varepsilon^h = w^h(p_\varepsilon^h) = w_1^h(p_\varepsilon^h) + i\, w_2^h(p_\varepsilon^h) \in \boldsymbol{V}^h$ is the unique weak solution of adjoint equation:

$$\begin{cases} -\Delta w_\varepsilon^h + w_\varepsilon^h = u_2^h(p_\varepsilon^h) & \text{in } \Omega, \\ \frac{\partial w_\varepsilon^h}{\partial n} + i\, w_\varepsilon^h = 0 & \text{on } \Gamma, \end{cases} \tag{31}$$

and $u_\varepsilon^h = u^h(p_\varepsilon^h) = u_1^h(p_\varepsilon^h) + i\, u_2^h(p_\varepsilon^h)$ is the solution of the problem (19) with p replaced by p_ε^h.

Before deriving an error estimate for the finite element solution p_ε^h of Problem 4.2, we note that for any $p \in Q$,

$$|||w(p) - w^h(p)|||_{1,\Omega} \le c\, h\, (\|p\|_{0,\Omega_0} + \|g_1\|_{1/2,\Gamma} + \|g_2\|_{1/2,\Gamma}), \tag{32}$$

$$|||w(p) - w^h(p)|||_{0,\Omega} \le c\, h^2\, (\|p\|_{0,\Omega_0} + \|g_1\|_{1/2,\Gamma} + \|g_2\|_{1/2,\Gamma}), \tag{33}$$

where $w(p) \in \mathbf{V}$ and $w^h(p) \in \mathbf{V}^h$ are the solutions of the problems (16) and (31), with p_ε and p_ε^h replaced by p in both. The bounds (32) and (33) are proved by arguments similar to those for (21) and (22).

Next we give an error estimate for the light source function p_ε w.r.t. h as follows.

Theorem 4.4 *Let $p_\varepsilon \in Q_{ad}$ be the solution of Problem 2.3 and $p_\varepsilon^h \in Q_{ad}^h$ be the solution of Problem 4.2. Then*

$$\|p_\varepsilon - p_\varepsilon^h\|_{0,\Omega_0} \le c\,(\varepsilon^{-1}\,h^2 + \varepsilon^{-1/2}\,h^{1/2}\,E^h(p_\varepsilon)^{1/2}), \tag{34}$$

where $E^h(p_\varepsilon) = \|\Pi^h p_\varepsilon - p_\varepsilon\|_{0,\Omega_0} = \inf_{q^h \in Q_{ad}^h} \|q^h - p_\varepsilon\|_{0,\Omega_0}$.

Proof. We give a sketch of proof; one may consult [17, Theorem 4.4] for details.

Let $\tilde{p}_\varepsilon^h \in Q_{ad}^h$ be the unique solution of Problem 4.2 with $J_\varepsilon^h(\cdot)$ replaced by $J_\varepsilon(\cdot)$. Then

$$(w_2(\tilde{p}_\varepsilon^h) + \varepsilon\,\tilde{p}_\varepsilon^h, q^h - \tilde{p}_\varepsilon^h)_{0,\Omega_0} \ge 0 \quad \forall\, q^h \in Q_{ad}^h, \tag{35}$$

with $\tilde{w}_\varepsilon := w(\tilde{p}_\varepsilon^h) = w_1(\tilde{p}_\varepsilon^h) + i\,w_2(\tilde{p}_\varepsilon^h) \in \mathbf{V}$ and $\tilde{u}_\varepsilon := u(\tilde{p}_\varepsilon^h) = u_1(\tilde{p}_\varepsilon^h) + i\,u_2(\tilde{p}_\varepsilon^h) \in \mathbf{V}$ being the unique weak solutions of BVPs:

$$\begin{cases} -\Delta\tilde{w}_\varepsilon + \tilde{w}_\varepsilon = u_2(\tilde{p}_\varepsilon^h) & \text{in } \Omega, \\ \frac{\partial\tilde{w}_\varepsilon}{\partial n} + i\,\tilde{w}_\varepsilon = 0 & \text{on } \Gamma, \end{cases}$$

and

$$\begin{cases} -\Delta\tilde{u}_\varepsilon + \tilde{u}_\varepsilon = \tilde{p}_\varepsilon^h\chi_{\Omega_0} & \text{in } \Omega, \\ \frac{\partial\tilde{u}_\varepsilon}{\partial n} + i\,\tilde{u}_\varepsilon = g_2 + i\,g_1 & \text{on } \Gamma, \end{cases}$$

respectively.

Replace q in (15) with $\tilde{p}_\varepsilon^h$ and $q^h \in Q_{ad}^h$ in (35) with $\Pi^h p_\varepsilon$, and add the resulting inequalities to get

$$\begin{aligned} \varepsilon\|\tilde{p}_\varepsilon^h - p_\varepsilon\|_{0,\Omega_0}^2 \le\ & (w_2(\tilde{p}_\varepsilon^h) + \varepsilon\,\tilde{p}_\varepsilon^h, \Pi^h p_\varepsilon - p_\varepsilon)_{0,\Omega_0} \\ & + (w_2(\tilde{p}_\varepsilon^h) - w_2(p_\varepsilon), p_\varepsilon - \tilde{p}_\varepsilon^h)_{0,\Omega_0}. \end{aligned} \tag{36}$$

Using (28), (29), and noticing $w_2(\tilde{p}_\varepsilon^h)\chi_{\Omega_0} \in H^1(\Omega_0)$, we have

$$\begin{aligned} (w_2(\tilde{p}_\varepsilon^h) + \varepsilon\,\tilde{p}_\varepsilon^h, \Pi^h p_\varepsilon - p_\varepsilon)_{0,\Omega_0} &= (w_2(\tilde{p}_\varepsilon^h) - \Pi^h w_2(\tilde{p}_\varepsilon^h)\chi_{\Omega_0}, \Pi^h p_\varepsilon - p_\varepsilon)_{0,\Omega_0} \\ &\le c\,h\,E^h(p_\varepsilon). \end{aligned} \tag{37}$$

Denote by $e_1^h = u_1(\tilde{p}_\varepsilon^h) - u_1(p_\varepsilon)$, $e_2^h = u_2(\tilde{p}_\varepsilon^h) - u_2(p_\varepsilon)$, $E_1^h = w_1(\tilde{p}_\varepsilon^h) - w_1(p_\varepsilon)$, and $E_2^h = w_2(\tilde{p}_\varepsilon^h) - w_2(p_\varepsilon)$. Then e_1^h satisfies

$$\begin{cases} -\Delta e_1^h + e_1^h = (\tilde{p}_\varepsilon^h - p_\varepsilon)\chi_{\Omega_0} & \text{in } \Omega, \\ \frac{\partial e_1^h}{\partial n} - e_2^h = 0 & \text{on } \Gamma, \end{cases} \tag{38}$$

e_2^h satisfies

$$\begin{cases} -\Delta e_2^h + e_2^h = 0 & \text{in } \Omega, \\ \frac{\partial e_2^h}{\partial n} + e_1^h = 0 & \text{on } \Gamma, \end{cases}$$

E_1^h satisfies

$$\begin{cases} -\Delta E_1^h + E_1^h = e_2^h & \text{in } \Omega, \\ \frac{\partial E_1^h}{\partial n} - E_2^h = 0 & \text{on } \Gamma, \end{cases} \tag{39}$$

and E_2^h satisfies

$$\begin{cases} -\Delta E_2^h + E_2^h = 0 & \text{in } \Omega, \\ \frac{\partial E_2^h}{\partial n} + E_1^h = 0 & \text{on } \Gamma. \end{cases}$$

Multiply (38) with E_2^h, integrate over Ω, and integrate by part to get

$$(E_2^h, \tilde{p}_\varepsilon^h - p_\varepsilon)_{0,\Omega_0} = -(e_1^h, E_1^h)_{0,\Gamma} - (e_2^h, E_2^h)_{0,\Gamma}. \tag{40}$$

Similarly, multiply (39) with e_2^h, integrate over Ω, and integrate by part to get

$$\|e_2^h\|_{0,\Omega}^2 = -(e_1^h, E_1^h)_{0,\Gamma} - (e_2^h, E_2^h)_{0,\Gamma}. \tag{41}$$

Combine (40) and (41) to get

$$(E_2^h, \tilde{p}_\varepsilon^h - p_\varepsilon)_{0,\Omega_0} = \|e_2^h\|_{0,\Omega}^2.$$

Therefore, from (36), (37) and the equality above, we obtain

$$\varepsilon \|\tilde{p}_\varepsilon^h - p_\varepsilon\|_{0,\Omega_0}^2 \le c\, h\, E^h(p_\varepsilon) - \|u_2(\tilde{p}_\varepsilon^h) - u_2(p_\varepsilon)\|_{0,\Omega}^2,$$

which gives

$$\|u_2(\tilde{p}_\varepsilon^h) - u_2(p_\varepsilon)\|_{0,\Omega}^2 + \varepsilon \|\tilde{p}_\varepsilon^h - p_\varepsilon\|_{0,\Omega_0}^2 \le c\, h\, E^h(p_\varepsilon)$$

and

$$\|\tilde{p}_\varepsilon^h - p_\varepsilon\|_{0,\Omega_0} \le c\, \varepsilon^{-1/2}\, h^{1/2}\, E^h(p_\varepsilon)^{1/2}. \tag{42}$$

Similarly, replace q^h in (30) with $\tilde{p}_\varepsilon^h$ and $q^h \in Q_{ad}^h$ in (35) with p_ε^h, and add the resulting inequalities to get

$$\begin{aligned} \varepsilon \|p_\varepsilon^h - \tilde{p}_\varepsilon^h\|_{0,\Omega_0}^2 &\le (w_2(\tilde{p}_\varepsilon^h) - w_2^h(p_\varepsilon^h), p_\varepsilon^h - \tilde{p}_\varepsilon^h)_{0,\Omega_0} \\ &\le (w_2(\tilde{p}_\varepsilon^h) - w_2(p_\varepsilon^h), p_\varepsilon^h - \tilde{p}_\varepsilon^h)_{0,\Omega_0} \\ &\quad + (w_2(p_\varepsilon^h) - w_2^h(p_\varepsilon^h), p_\varepsilon^h - \tilde{p}_\varepsilon^h)_{0,\Omega_0}. \end{aligned} \tag{43}$$

From (33), we have

$$|(w_2(p_\varepsilon^h) - w_2^h(p_\varepsilon^h), p_\varepsilon^h - \tilde{p}_\varepsilon^h)_{0,\Omega_0}| \le c\, h^2\, \|p_\varepsilon^h - \tilde{p}_\varepsilon^h\|_{0,\Omega_0}. \tag{44}$$

Moreover, with an argument similar to that used for (38)–(41), we have

$$(w_2(\tilde{p}_\varepsilon^h) - w_2(p_\varepsilon^h), p_\varepsilon^h - \tilde{p}_\varepsilon^h)_{0,\Omega_0} = -\|u_2(p_\varepsilon^h) - u_2(\tilde{p}_\varepsilon^h)\|_{0,\Omega}^2. \tag{45}$$

Then combine (43)–(45) to give

$$\|u_2(p_\varepsilon^h) - u_2(\tilde{p}_\varepsilon^h)\|_{0,\Omega}^2 + \varepsilon \|p_\varepsilon^h - \tilde{p}_\varepsilon^h\|_{0,\Omega_0}^2 \le c\, h^2\, \|p_\varepsilon^h - \tilde{p}_\varepsilon^h\|_{0,\Omega_0}$$

and

$$\|p_\varepsilon^h - \tilde{p}_\varepsilon^h\|_{0,\Omega_0} \le c\, \varepsilon^{-1}\, h^2. \tag{46}$$

Consequently, from (42) and (46) as well as triangle inequality

$$\|p_\varepsilon^h - p_\varepsilon\|_{0,\Omega_0} \le \|p_\varepsilon^h - \tilde{p}_\varepsilon^h\|_{0,\Omega_0} + \|\tilde{p}_\varepsilon^h - p_\varepsilon\|_{0,\Omega_0},$$

we obtain the error bound (34) and the proof is completed. ■

5. An algorithm

Let n be the number of the nodes of triangulation $\mathcal{T}_h$, and $\{\varphi_l\}_{l=1}^n \subset V^h$ be the nodal basis functions of the linear finite element space V^h associated with the grid points $\{x_l\}_{l=1}^n$. Then $u^h \in \mathbf{V}^h$ can be written as $u^h = \sum_{l=1}^n u_l\,\varphi_l$, with $u_l = u^h(x_l) \in \mathbb{C}$. Moreover, for a triangulation $\mathcal{T}_h$, denote by N the number of elements in $\overline{\Omega}_0$. Then $q^h \in Q^h$ can be written as $q^h = \sum_{T_j \subset \overline{\Omega}_0} q_j\,\chi_{T_j}$ with $q_j = q^h(\hat{x}_j)$, $1 \le j \le N$, where $\hat{x}_j$ is an inner point (e.g., centroid) of element T_j and χ_{T_j} is the characteristic function of $T_j \in \mathcal{T}_h$. As a result, the discrete problem (19) reduces to the following algebra problem:

$$(K + M + i\,C)\,u = B\,p + i\,b_1 + b_2, \tag{47}$$

where

$$\begin{array}{ll}
K = (k_{ls})_{n\times n}, & k_{ls} = \int_\Omega \nabla\varphi_s \cdot \nabla\varphi_l \,\mathrm{d}x,\\
M = (m_{ls})_{n\times n}, & m_{ls} = \int_\Omega \varphi_s\,\varphi_l \,\mathrm{d}x\\
C = (c_{ls})_{n\times n}, & c_{ls} = \int_\Gamma \varphi_s\,\varphi_l \,\mathrm{d}s,\\
B = (b_{lj})_{n\times N}, & b_{lj} = \int_{T_j} \varphi_l \,\mathrm{d}x,\\
b_1 = (b_{1,l})_{n\times 1}, & b_{1,l} = \int_\Gamma g_1\,\varphi_l \,\mathrm{d}s,\\
b_2 = (b_{2,l})_{n\times 1}, & b_{2,l} = \int_\Gamma g_2\,\varphi_l \,\mathrm{d}s,\\
u = (u_l)_{n\times 1}, & p = (p_j)_{N\times 1},\\
l, s = 1, 2, \cdots, n, & j = 1, 2, \cdots, N.
\end{array}$$

We note that the same symbol u is used for a function in space $\mathbf{V}$ or a vector in $\mathbb{C}^n$; no confusion is expected from the context. This is also true for symbols p and u_1, u_2, w_1, w_2 and p_ε below.

Let $u = u_1 + i\,u_2$ with $u_1, u_2 \in \mathbb{R}^n$. Then (47) reduces further to the system

$$\begin{cases} (K + M)\,u_1 - C\,u_2 = B\,p + b_2,\\ C\,u_1 + (K + M)\,u_2 = b_1. \end{cases} \tag{48}$$

Similarly, finding a weak solution of (31) reduces to finding $w = w_1 + i\,w_2 \in \mathbb{C}^n$ with $w_1, w_2 \in \mathbb{R}^n$ such that

$$\begin{cases} (K + M)\,w_1 - C\,w_2 = M\,u_2,\\ C\,w_1 + (K + M)\,w_2 = 0. \end{cases} \tag{49}$$

Denote by $M_0 = \mathrm{diag}(|T_{k_1}|, |T_{k_2}|, \cdots, |T_{k_N}|)$ the N dimensional diagonal matrix, $|T_{k_j}|$ being the measure of T_{k_j}. Set $Q_{ad}^N = \{q \in \mathbb{R}^N \mid \sum_{T_j \subset \overline{\Omega}_0} q_j \chi_{T_j} \in Q_{ad}^h\}$ and define $J_\varepsilon^N(p) = \frac{1}{2}u_2^t\,M\,u_2 + \frac{\varepsilon}{2}p^t\,M_0\,p$, where the superscript t signifies a transposition operation. Then Problem 4.2 reduces further to the following quadratic programming.

Problem 5.1 *Find $p_\varepsilon \in Q_{ad}^N$ such that*

$$J_\varepsilon^N(p_\varepsilon) = \inf_{p \in Q_{ad}^N} J_\varepsilon^N(p).$$

Correspondingly, the optimality condition (30) reduces to

$$(\Pi^N w_2(p_\varepsilon) + \varepsilon\, p_\varepsilon)^t\, M_0\, (q - p_\varepsilon) \geq 0 \quad \forall\, q \in Q_{ad}^N, \tag{50}$$

where $w_2(p_\varepsilon) \in \mathbb{R}^n$ is the solution of (48) and (49) with p replaced by p_ε, $\Pi^N = (\pi_{jl})_{N\times n}$ with

$$\pi_{jl} = \begin{cases} \frac{1}{d+1} & x_l \in T_j \subset \overline{\Omega}_0, \\ 0 & \text{otherwise.} \end{cases}$$

Consequently, numerically solving the original inverse source problem reduces to solving the linear algebraic systems (48), (49) and (50) for $u_1, u_2, w_1, w_2 \in \mathbb{R}^n$ and $p_\varepsilon \in \mathbb{R}^N$. Denote by P_{ad} a projection operator from Q onto Q_{ad} and P_{ad}^N its discrete one under our finite element context. We introduce the following iterative algorithm.

Algorithm 5.2 *1. Given precision $\epsilon > 0$. Let $p^0 = 0 \in \mathbb{R}^N$ and set $k = 0$.*

2. Solve (48) with p replaced by p^k to $u_2^k = u_2$.

3. Solve (49) with u_2 replaced by u_2^k to $w_2^k = w_2$.

4. Compute $p_\varepsilon^{k+1} = P_{ad}^N\left(-\Pi^N w_2^k/\varepsilon\right)$.

5. If $e^k = \|p_\varepsilon^{k+1} - p_\varepsilon^k\| \leq \epsilon$, stop; otherwise, set $k = k + 1$ and turn to Step 2.

Convergence behavior of Algorithm 5.2 depends on the regularization parameter ε. For applications, Q_{ad} usually takes one of three forms: Case 1, $Q_{ad} = Q$; Case 2, $Q_{ad} = \{q \in Q \mid q \geq 0 \text{ a.e. in } \Omega_0\}$; Case 3, $Q_{ad} = \{q \in Q \mid \underline{q} \leq q \leq \overline{q} \text{ a.e. in } \Omega_0\}$ with $\underline{q}, \overline{q} \in C(\overline{\Omega}_0)$. In these cases, P_{ad}^N has simpler forms: $\forall\, p \in \mathbb{R}^N$,

$$P_{ad}^N(p) = \begin{cases} p & \text{Case 1,} \\ \max\{0, p\} & \text{Case 2,} \\ \max\{\underline{q}, \min\{\overline{q}, p\}\} & \text{Case 3,} \end{cases}$$

where $\underline{q}_j = \max_{x\in T_j} \underline{q}(x)$ and $\overline{q}_j = \min_{x\in T_j} \overline{q}(x)$.

Remark 5.3 *In the case $Q_{ad} = Q$, the iteration above could be avoided. In fact, in this case, (50) reduces to $p_\varepsilon = -\Pi^N w_2/\varepsilon$. Use this expression in (48) and (49) to get*

$$\begin{cases} (K + M)\, u_1 - C\, u_2 + \frac{1}{\varepsilon} B\, \Pi^N\, w_2 = b_2, \\ C\, u_1 + (K + M)\, u_2 = b_1, \\ -M\, u_2 + (K + M)\, w_1 - C\, w_2 = 0, \\ C\, w_1 + (K + M)\, w_2 = 0. \end{cases} \tag{51}$$

Once w_2 is computed from the system (51), we obtain $p_\varepsilon = -\Pi^N w_2/\varepsilon$.

6. Numerical results

We present in this section some numerical results based on our CCBM. The goal is to demonstrate its feasibility for the inverse source problems. Let Ω be the problem domain and mesh parameter h be the maximal diameter of the elements in the partition $\mathcal{T}_h$. For finite-element spaces V^h and Q^h, we use continuous piecewise linear functions and piecewise constant functions corresponding to the partitions $\mathcal{T}_h$. In the following, we compute the approximate source function p_ε^h for different grid parameter h, different regularization parameter ε and noise level δ. In the examples, if not given, the boundary measurements g_1, which may or may not include noise, are obtained by solving the BVP (2) on a rather small mesh for given p and g_2.

In the following, for 2D domain, a triangular mesh is produced through matlab code "initmesh" which uses a Delaunay triangulation algorithm. The triangular mesh are refined through matlab code "refinemesh" which either divides all edges of the selected triangles in half (regular refinement), or divides the longest edge in half (longest edge refinement). For 3D domain, a tetrahedral mesh is produced and refined through a COMSOL Multiphysics soft. The resulting linear algebra system (51) is solved by the biconjugate gradient method. It is known that the regularization parameter ε has an important effect on the accuracy of the reconstructed light source function.

We also note that the numerical results below are computed for optimal regularization parameters. In the literature, there are many methods developed for choosing parameters properly, such as the discrepancy principle (DP), L-curve rule and so on. We refer to [19] for some comments on the choice of these regularization parameters. In this section, all optimal regularization parameters are chosen approximately by sweeping them from 1 to $1 \times 10^{-1}, 1 \times 10^{-2}, 1 \times 10^{-3}, \cdots$.

We define three evaluation indicators:
(1) L^2-norm relative error in approximate solution p_ε^h,

$$\mathrm{Err}(p) := \|p_\varepsilon^h - p\|_{0,\Omega_0};$$

(2) mean value of approximate solution p_ε^h,

$$\mathrm{Mean}(p) := \frac{1}{N} \sum_{T_j \subset \bar{\Omega}_0} p_j$$

with N being the number of elements in $\bar{\Omega}_0$; $p_j = p_\varepsilon^h \mid_{T_j}$;
(3) variance of approximate solution p_ε^h,

$$\mathrm{Var}(p) := \frac{1}{N} \sum_{T_j \subset \bar{\Omega}_0} (p_j - \mathrm{Mean}(p))^2.$$

Example 1 In the first example, the problem domain $\Omega = \{(x, y) \in \Omega \mid x^2 + y^2 < 1\}$. Let $g_2 = 1$ on Γ, and the exact source function

$$p = \begin{cases} 1, & \text{if } (x - 0.55)^2 + (y - 0.45)^2 \leq 0.1^2, \\ 0, & \text{otherwise.} \end{cases}$$

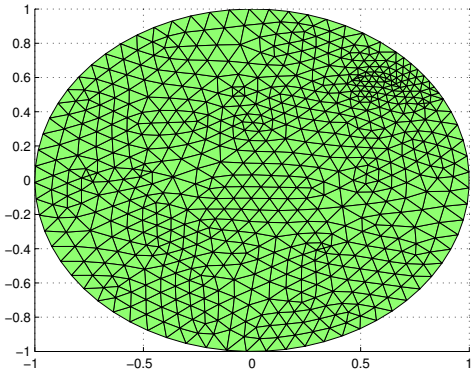

Figure 1. Sample Delaunay triangulations (Example 1)

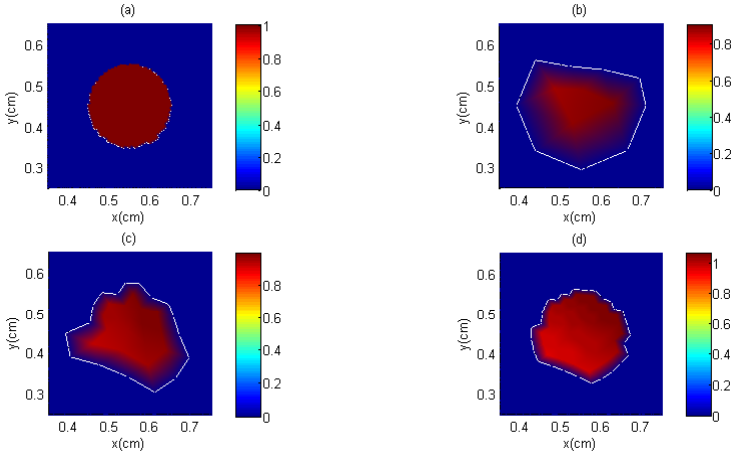

Figure 2. Exact p and reconstructed p_ε^h for noise-free g_1 (Example 1)

Table 1. Three evaluation indicators for noise-free g_1 (Example 1)

h	Err(p)	Mean(p)	Var(p)
ne=322, n=180	4.9697e-2	0.8868	2.0504e-4
ne=1288, n=681	3.5089e-2	0.9607	3.4858e-4
ne=5152, n=2649	2.7164e-2	1.0171	6.79291e-4

Delaunay triangles are used for the domain triangulations and a sample is plotted in Figure 1. Data g_1 is computed on a mesh with 10449 elements and 20608 nodes. Then Algorithm 5.2 is applied for obtaining an approximate source function p_ε^h. Reconstructed source functions on different meshes are plotted in Figure 2. In Figure 2, the first subgraph 2(a) is the exact source function p; subgraph 2(b) is the source function p_ε^h computed on the mesh with 322 elements and 180 nodes; subgraph 2(c) represents p_ε^h reconstructed on the mesh with 1288 elements and 681 nodes; subgraph 2(d)

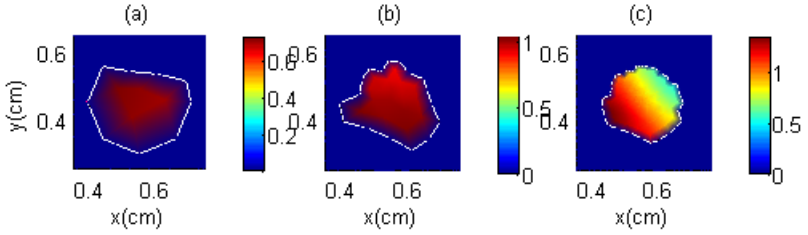

Figure 3. p_ε^h for measurement g_1 with 10% random noise (Example 1)

Table 2. Three evaluation indicators for measurement g_1 with 10% random noise (Example 1)

h	Err(p)	Mean(p)	Var(p)
ne=322, n=180	1.2474e-1	0.7183	1.4092e-4
ne=1288, n=681	2.8434e-2	0.9698	1.0440e-3
ne=5152, n=2649	1.9291e-1	0.9123	3.7414e-2

represents p_ε^h reconstructed on the mesh with 5152 elements and 2649 nodes. The optimal regularization parameters for three reconstructions are 2×10^{-4}, 3×10^{-4} and 4×10^{-5} respectively. Moreover, for each reconstruction, we compute the values of three evaluation indicators 'Err(p)', 'Mean(p)' and 'Var(p)' defined above, and list them in Table 1. Here and below, 'ne' and 'n' stand for the number of elements and the number of nodes of a triangulation over $\bar{\Omega}$. Figure 2 and Table 1 show that reconstructions are satisfactory and the solution accuracy improves as the mesh is refined. 'Var(p)' in Table 1 also indicates that like true constant source function p, p_ε^h is relatively flat.

To measure the stability of our proposed reconstruction framework, we add a 10% uniformly distributed noise to g_1 and repeat the numerical experiment. Reconstructed source functions on three corresponding meshes are shown in Figure 3. Specifically, subgraphs 3(a), 3(b) and 3(c) are computed source functions over mesh with 322 triangles and 180 nodes, mesh with 1288 triangles and 681 nodes, and mesh with 5152 triangles and 2649 nodes, respectively. The optimal regularization parameters for three reconstructions are 2×10^{-3}, 1×10^{-3} and 2×10^{-4} respectively. Again the values of three

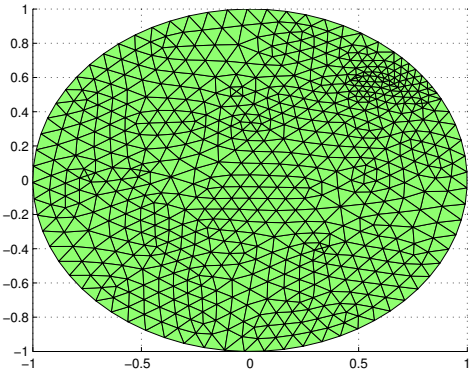

Figure 4. Sample Delaunay triangulations (Example 2)

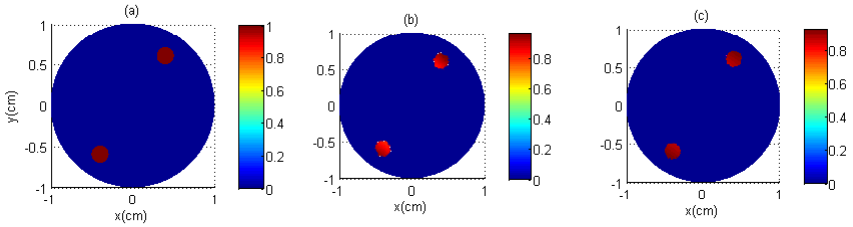

Figure 5. Exact p and reconstructed p_ε^h for noise-free g_1 (Example 2)

evaluation indicators 'Err(p)', 'Mean(p)' and 'Var(p)' are computed and listed in Table 2. We conclude from Figure 3 and Table 2 that the reconstruction is stable. In addition, Figure 3 and Table 2 suggest that for measurement data with noise, over-refinement of the mesh is not advisable.

Example 2 In the second example, let Ω and $g_2 = 1$ be the same as Example 1. Differently, now the exact source function

$$p = \begin{cases} 1, & \text{if } (x-0.4)^2 + (y \pm 0.6)^2 \le 0.1^2, \\ 0, & \text{otherwise} \end{cases}$$

We plot p in subgraph 5(a) of Figure 5.

Again Delaunay triangles are used for the domain triangulations and a sample is plotted in Figure 4, and g_1 is computed on a mesh with 42701 elements and 85056 nodes. Then numerical simulations are implemented for triangulations with different meshsize. Approximate source function p_ε^h computed over mesh with 1329 elements

Table 3. Three evaluation indicators for measurement g_1 without noise (Example 2)

h	Err(p)	Mean(p)	Var(p)
ne=1329, n=687	1.0733e-1	0.8873	1.0734e-3
ne=5316, n=2702	2.8194e-2	1.0197	3.3425e-4

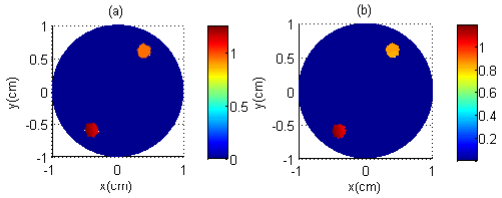

Figure 6. p_ε^h for measurement g_1 with 5% random noise (Example 2)

and 687 nodes is shown in subgraph 5(b) of Figure 5. Subgraph 5(c) of Figure 5 is p_ε^h for triangulation with 5316 triangles and 2702 nodes. The corresponding optimal regularization parameters are 2×10^{-5} and 3×10^{-4} respectively. Similarly, the values of three evaluation indicators 'Err(p)', 'Mean(p)' and 'Var(p)' are computed and listed in Table 3. We have same conclusions about feasibility and accuracy as Example 1.

Table 4. Three evaluation indicators for measurement g_1 with 5% random noise (Example 2)

h	Err(p)	Mean(p)	Var(p)
ne=1329, n=687	1.2009e-1	1.0604	1.4318e-2
ne=5316, n=2702	1.3342e-1	0.9730	1.9604e-2

To measure the stability of our proposed reconstruction framework, we add a 5% uniformly distributed noise to g_1 and repeat the numerical experiment. Reconstruction results are reported in Figure 6 and Table 4. In Figure 6, subgraph 6(a) is the source function over mesh with 1329 triangles and 687 nodes while subgraph 6(b) is the computed source function for mesh with 5316 triangles and 2702 nodes. Both reconstructions have the same optimal regularization parameter: 1×10^{-3}. Again the values of three evaluation indicators 'Err(p)', 'Mean(p)' and 'Var(p)' are computed and listed in Table 4. We conclude again from Figure 6 and Table 4 that the reconstruction is stable, and for measurement data with noise, it is better not to over-refine the mesh.

Example 3 In our last example, we consider a 3D problem. Let the problem domain

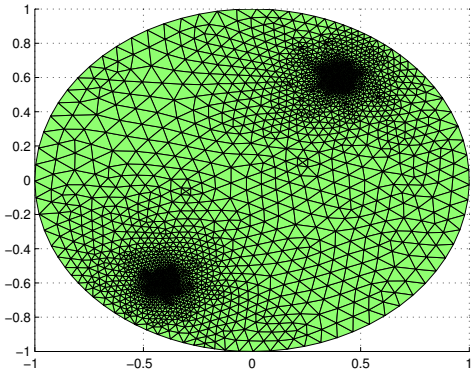

Figure 7. Triangulation of Ω (Example 3)

be a sphere centered at origin with radius 10:

$$\Omega = \{(x, y, z) \in \mathbb{R}^3 \mid x^2 + y^2 + z^2 < 10^2\},$$

and a sphere light source $p = 1$, centered at $(-5, -5, 5)^T$ with radius 2, be embedded into Ω. Set $g_2 = |x + y + z|$ on Γ. Figure 7 sketches a tetrahedral triangulation of the 3D domain. Moreover, for given exact source function p, the measurement data g_1 is computed on a mesh with 64349 elements and 11838 nodes.

Table 5. Three evaluation indicators for measurement g_1 without noise (Example 3)

h	Err(p)	Mean(p)	Var(p)
ne=1329, n=687	2.4848e-1	0.9831	6.1785e-2
ne=5316, n=2702	2.2926e-1	0.9149	4.3079e-2

Table 6. Three evaluation indicators for measurement g_1 with 10% random noise (Example 3)

h	Err(p)	Mean(p)	Var(p)
ne=2472, n=543	3.3607e-1	0.8704	5.9959e-2
ne=5316, n=2702	2.8753e-1	0.9605	7.5677e-2

Then we apply Algorithm 5.2 again to obtain the approximate solution p_ε^h. We implement the reconstruction on two different meshes: the mesh with 2472 tetrahedrons and 543 nodes; the mesh with 5316 tetrahedrons and 2702 nodes. Since p_ε^h here is a three dimensional function, we do not display it in figure. Instead, we list the values of three evaluation indicators 'Err(p)', 'Mean(p)' and 'Var(p)' defined above to judge the behaviors of reconstructions. Results for noise-free measurement g_1 is report in Table 5 while Results for g_1 with 10% is report in Table 6. We note that all optimal regularization parameters for the four reconstructions are $\varepsilon = 2 \times 10^{-2}$. Tables 5 and

6 show that although the error is bigger than those in Example 1 and Example 2, the results here are still acceptable.

All numerical results given above are implemented for Case 1: $Q_{ad} = Q$. Using Algorithm 5.2, we repeat the experiments for Case 2: $Q_{ad} = \{q \in Q \mid q \geq 0 \text{ a.e. in } \Omega_0\}$ and Case 3: $Q_{ad} = \{q \in Q \mid 0 \leq q \leq 10 \text{ a.e. in } \Omega_0\}$, and the reconstructed results are similar to those in Case 1. In summary, we conclude that Algorithm 5.2 is feasible and effective.

7. Conclusions

A classical partial differential equation inverse source problem often involves Neumann data and Dirichlet data. Unlike the existing methods, in this paper we propose a method using both Neumann and Dirichlet data in a single boundary value problem. We match data in the problem domain rather than on the boundary. Tikhonov regularization methods and finite element methods are applied for obtaining a discrete stable source function. Theoretical and numerical results show that the proposed method is feasible and effective. As is known, a priori information about source function is helpful and has great impact on the solution accuracy for our reconstruction model. Moreover, the regularization parameter plays an important role in the reconstruction, and affects the performance and convergence of Algorithm 5.2. Current research efforts include using an optimal regularization parameter computed from many parameter selecting methods, and application of the coupled complex boundary method to inverse parameter problems as well as time-dependent inverse problems.

Acknowledgments

We express our gratitude to the anonymous reviewers whose valuable comments and suggestions lead to an improvement of the manuscript. The work of the first author was supported by the Key Project of the Major Research Plan of NSFC (Grant No. 91130004). The work of the second author was supported by the natural science foundation of Jiangsu Province (Grant No. BK20130780) and the Fundamental Research Funds for the Central Universities (Grant No. NS2014078). The work of the third author was supported by grants from the Simons Foundation.

References

[1] Afraites L, Dambrine M and Kateb D 2007 Conformal mappings and shape derivatives for the transmission problem with a single measurement *Numer. Func. Anal. Opt.* **28** 519–551

[2] Afraites L, Dambrine M and Kateb D 2008 On second order shape optimization methods for electrical impedance tomography *SIAM J. Control Optim.* **47** 1556–1590

[3] Alber Y and Ryazantseva I 2006 *Nonlinear Ill-posed Problems of Monotone Type* (Netherlands: Springer)

[4] Atkinson K and Han W 2009 *Theoretical Numerical Analysis: A Functional Analysis Framework* 3rd edn (New York: Springer-Verlag)

[5] Bakushinsky A B and Kokurin M Yu 2004 *Iterative Methods for Approximate Solution of Inverse Problems* (Netherlands: Springer)

[6] Chavent G and Kunisch K 1994 Convergence of Tikhonov regularization for constrained ill-posed inverse problems *Inverse Probl.* **10** 63–76

[7] Cheng X L, Gong R F and Han W 2008 A new general mathematical framework for bioluminescence tomography *Comput. Methods Appl. Mech. Engrg.* **197** 524–535

[8] Chouli M and Yamamoto M 2004 Conditional stability in determing a heat source *J. Inverse Ill-posed Probl.* **12** 233–243

[9] Ciarlet P G 1978 *The Finite Element Method for Elliptic Problems* (Amsterdam: North-Holland)

[10] Dautray R and Lions J L 1988 *Mathematical Analysis and Numerical Methods for Science and Technology Vol. 2* (Berlin: Springer)

[11] Doicu A, Trautmann T and Schreier F 2010 *Numerical Regularization for Atmospheric Inverse Problems* (Heidelberg: Springer-Verlag)

[12] Engl H W, Kunisch K and Neubauer A 1989 Convergence rates for Tikhonov regularization of non-linear ill-posed problems *Inverse Probl.* **5** 523–540

[13] Feng J *et al* 2012 Total variation regularization for bioluminescence tomography with the split Bregman method *Appl. Opt.* **51** 4501–4512

[14] Guo W *et al* 2002 Efficient sparse reconstruction algorithm for bioluminescence tomography based on duality and variable splitting *Appl. Opt.* **51** 5676–5685

[15] Grisvard P 1985 *Elliptic Problems in Nonsmooth Domains* (Boston: Pitman)

[16] Glashoff K and Gustafson S A 1983 *Linear Optimization and Approximation: An Introduction to the Theoretical Analysis and Numerical Treatment of Semi-infinite Programs* (New York: Springer-Verlag)

[17] Gong R F and Cheng X L An optimal finite element error estimate for an inverse problem in multispectral bioluminescence tomography *IMA J. Appl. Math.* to appear

[18] Hadamard J 1923 *Lectures on the Cauchy's Problem in Linear Partial Differential Equations* (London: Yale University Press)

[19] Hämarik U, Palm R and Raus T 2012 A family of rules for parameter choice in Tikhonov regularization of ill-posed problems with inexact noise level *J. Comput. Appl. Math.*, **236** 2146–2157

[20] Han W, Cong W X and Wang G 2006 Mathematical theory and numerical analysis of bioluminescence tomography *Inverse Probl.*, **22** 1659–1675

[21] Han W, Kazmi K, Cong W X and Wang G 2007 Bioluminescence tomography with optimized optical parameters *Inverse Probl.* **23** 1215–1228

[22] He X *et al* 2011 Sparse regularization-based reconstruction for bioluminescence tomography using a multilevel adaptive finite element method, *Int. J. Biomed. Imag.* **203537** 11 pages.

[23] Isakov V 1990 *Inverse Source Problems* (Providence: American Mathematical Society)

[24] Isakov V 2006 *Inverse Problems for Partial Differential Equations* 2nd ed (New York: Springer)

[25] Kohm K and Vogelius M 1984 Determining conductivity by boundary measurements *Comm. Pure Appl. Math.* **37** 289-298.

[26] Kaipio J and Somersalo E 2005 *Statistical and Computational Inverse Problems* (New York:

Springer-Verlag)
[27] Liu K *et al* 2010 A fast bioluminescent source localization method based on generalized graph cuts with mouse model validations *Opt. Express* **18** 3732–3745
[28] Liu Y, Zhang X and Lu M W 2005 A meshless method based on least-squares approach for steady- and unsteady-state heat conduction problems *Numerical Heat Transfer, Part B* **47** 257–275
[29] Lv Y J *et al* 2006 A multilevel adaptive finite element algorithm for bioluminescence tomography *Opt. Express* **14** 8211–8223
[30] Martin T J and Dulikravich G S 1996 Inverse determination of boundary conditions and sources in steady heat conduction with heat generation *Journal of Heat Transfer* **118** 546–554
[31] Shi J, Tian J and Xu M 2008 Reconstruction-oriented multigrid finite element algorithm on bioluminescence tomography incorporating priori information *Commun. Numer. Meth. Engng* DOI: 10.1002/cnm.1157
[32] Song S J and Huang J G 2012 Solving an inverse problem from bioluminescence tomography by minimizing an energy-like functional *J. Comput. Anal. Appl.* **14** 544–558
[33] Tikhonov A N and Arsenin V Y 1977 *Solutions of Ill-Posed Problems* (New York: Wiley)
[34] Wang T *et al* 2010 Overlap domain decomposition method for bioluminescence tomography (BLT) *Commun. Numer. Meth. Engng.* **26** 511–523